Journal of Orthodontic and Periodontal Biomaterials Research

2024, Volume 4, Issue 1, Page No: 54-66

Available online at: https://galaxypub.co/

Galaxy Publication

Mechanical Properties and Antimicrobial Performance of Chitosan-Coated Orthodontic Elastomeric Modules

Maria Q. Gonzalez[1], Carlos J. Rodriguez[1], Daniela Vega[1]*, Camila H. Vega[2], Maria G. Torres[2], Valentina Hernandez[2]

[1]Department of Orthodontics and Dentofacial Orthopedics, College of Dental Medicine, Complutense University of Madrid, Madrid, Mexico.
[2]Department of Orthodontics, School of Dentistry, University of Buenos Aires, Buenos Aires, Mexico.

***E-mail** ✉ daniela.vega8@gmail.com

Received: 12 January 2024; **Revised:** 29 March 2024; **Accepted:** 05 April 2024

ABSTRACT

Orthodontic devices can disturb the balance of oral biofilms, increasing plaque accumulation and the risk of oral disease, with elastomeric modules (EMs) particularly prone to bacterial colonization due to their material properties. Surface modifications have been explored to limit microbial growth. This study investigated the mechanical performance, antibacterial effects, and cytocompatibility of chitosan-based coatings applied to EMs. EMs were coated with either chitosan (CS) or chitosan cross-linked with glutaraldehyde (CS-GTA), while uncoated modules served as controls. The coated modules underwent characterization via Fourier transform infrared (FTIR) and Raman spectroscopy and were subjected to tensile testing to evaluate mechanical properties. Antimicrobial activity was determined through colony-forming unit (CFU) counts, and cytocompatibility was assessed using gingival fibroblasts and the MTT assay. Statistical analyses included ANOVA, Tukey, Kolmogorov–Smirnov, and Kruskal–Wallis tests. Raman analysis confirmed characteristic molecular vibrations of the chitosan coatings. Mechanical testing indicated significant differences among materials, with CS-GTA differing notably from controls, as verified by Tukey post hoc analysis; however, yield stress values did not differ significantly. Both coated groups exhibited lower CFU counts compared to uncoated EMs, and cell viability remained high, averaging 85% for CS and 89% for CS-GTA coatings. CS and glutaraldehyde-cross-linked CS coatings were successfully prepared for EMs without compromising their mechanical integrity. Both coatings effectively suppressed bacterial growth, with no significant difference in antibacterial efficacy between the two coating types.

Keywords: Oral biofilm, Chitosan, Glutaraldehyde, Orthodontics, Elastomeric modules

How to Cite This Article: Gonzalez MQ, Rodriguez CJ, Vega D, Vega CH, Torres MG, Hernandez V. Mechanical Properties and Antimicrobial Performance of Chitosan-Coated Orthodontic Elastomeric Modules. J Orthod Periodontal Biomater Res. 2024;4(1):54-66. https://doi.org/10.51847/Du1e2VKckr

Introduction

The oral cavity hosts a dynamic biofilm, composed of a complex array of microorganisms that attach to teeth and gingival surfaces [1, 2]. In a healthy state, this microbiome maintains oral equilibrium [3]; however, fixed orthodontic devices disrupt this balance by creating additional plaque-retentive areas, promoting bacterial accumulation, and complicating oral hygiene practices [4]. This disturbance favors the growth of pathogenic species [5], which can lead to enamel demineralization, early white spot lesions, and periodontal complications [2, 6]. With the rising number of individuals seeking orthodontic treatment [7], maintaining oral hygiene remains challenging, even with improvements in appliance design [4, 6, 8], and crowded dentition—the most prevalent form of malocclusion [9]—further complicates cleaning efforts.

Elastomeric modules (EMs) are routinely employed in orthodontics to attach brackets to archwires and deliver the forces necessary for tooth movement [10]. These modules are popular due to their simplicity of application, patient comfort, versatility, and cost-effectiveness [11]. However, their polyurethane surfaces readily support microbial adhesion, which can disturb oral microbial balance [12, 13]. To counteract bacterial colonization, Jeon *et al.* integrated chlorhexidine into EMs to provide sustained antimicrobial effects [14], while Hernández-Gomora *et al.* incorporated silver nanoparticles into the elastomer matrix for similar outcomes [15].

Chitosan (CS) is a naturally derived biopolymer valued in dental applications for its biocompatibility, biodegradability, and antimicrobial properties [16–18]. It is obtained by deacetylating chitin, a structural polysaccharide found in crustacean shells, converting acetyl groups into amines [19–23]. The antimicrobial effect of CS arises from its positively charged molecules, which interact with negatively charged bacterial membranes, causing membrane disruption and leakage of cellular contents [24, 25]. D'Almeida *et al.* demonstrated that titanium alloys coated with chitosan significantly inhibited the growth of E. coli and S. aureus [26], and Uysal *et al.* found that chitosan-containing toothpaste prevented enamel demineralization in orthodontic patients more effectively than non-fluoridated options [27].

Glutaraldehyde (GTA) is widely recognized for its disinfectant properties [28]. Its incorporation into polymers can enhance crosslinking, thereby improving mechanical stability and providing antimicrobial activity due to its molecular structure [23, 29]. GTA was included in this study as both a reference for antibacterial performance and as a potential enhancer of antibiofilm properties.

Assessing cell viability is crucial to ensure that biomaterials in contact with oral tissues—such as mucosa, gingiva, or teeth—do not provoke adverse immune reactions [27]. The MTT assay is commonly employed for this purpose [30]. Controlling pathogenic biofilms remains a significant concern in orthodontic care with fixed appliances.

The objective of this study was to develop a chitosan coating for EMs, evaluate its antimicrobial and mechanical performance, and examine its impact on cell viability.

Materials and Methods

Chitosan coating of elastomeric modules

Translucent EMs (TP Orthodontics, TP Orthodontics, Inc., La Porte, IN, USA) and chitosan (Sigma-Aldrich, St. Louis, MO, USA) with a molecular weight of 223.332 g/mol and 70–80 percent deacetylation were used. To prepare the experimental solution, 100 mg of chitosan was dissolved in 30 mL of 0.4 M acetic acid (pH 4.5), yielding a 33.33 percent w/v solution. The EMs were first subjected to spin-coating at 450 RPM at room temperature for 2 hours, then immersed in the chitosan solution for 1 minute. Afterward, the modules were air-dried at room temperature for 120 hours, neutralized with NaOH, rinsed thoroughly with water, and allowed to dry for another 24 hours at room temperature **(Figure 1)**.

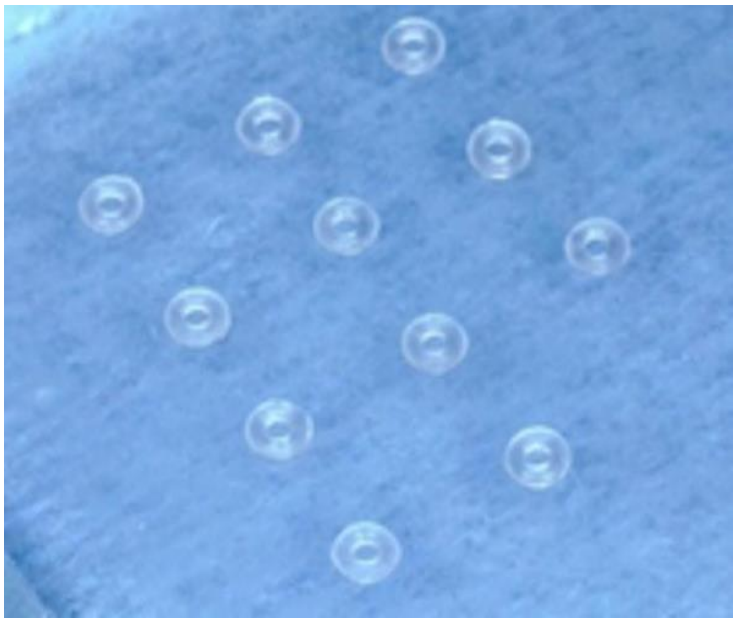

Figure 1. Chitosan-coated elastomeric modules

A second formulation was created using the same procedure, but incorporating 75 mL of 25% grade II glutaraldehyde (GTA; molar mass: 100.11 g/mol). Following coating with either chitosan alone or the chitosan–GTA mixture, the elastomeric modules were neutralized in a 5 percent sodium hydroxide (NaOH) solution, rinsed thoroughly with distilled water, and allowed to dry at room temperature for 24 hours. Modules left uncoated were designated as the control group for comparative analyses.

Physicochemical and mechanical characterization

To assess chemical composition, the coated EMs were examined by Fourier-transform infrared spectroscopy with attenuated total reflectance (FTIR-ATR) using a Nicolet 8700 spectrophotometer (Thermo Fisher Scientific Inc., Milwaukee, WI, USA). Measurements were performed over a spectral range of 4000–650 cm^{-1} using a zinc selenide crystal detector, at 4 cm^{-1} resolution, with an average of 50 scans per sample.

Raman spectroscopy analysis was carried out using an InVia™ Raman Microscope (Renishaw plc, Wotton-under-Edge, Gloucestershire, UK), employing a 633 nm laser at 50 percent power. Each module was scanned from 100 to 3200 cm^{-1} with two accumulations, using an 1800 grating, a 50× objective, and 10-second exposure times.

The mechanical performance of the modules was tested on a Mini Shimadzu universal testing machine (Shimadzu Corporation, Kyoto, Japan) following ASTM D624 standards for tensile strength. A 1 kN load cell and a crosshead speed of ten millimeters per minute were used. Due to the geometry of the modules, each EM was secured in a custom holder made from 0.3 millimeters orthodontic stainless-steel wire, adapted to fit the machine's grips **(Figure 2)**. Testing continued until fracture occurred, and data were collected to calculate key mechanical parameters, including yield deformation (YD), yield stress (YS), maximum deformation (MD), and maximum stress (MS).

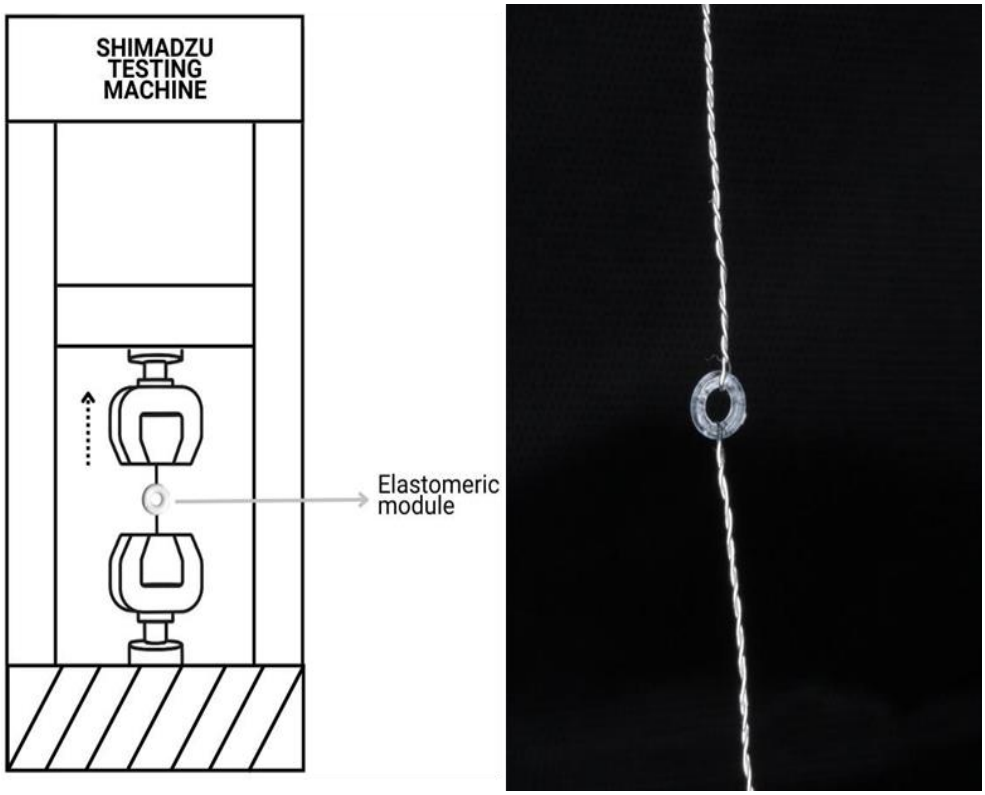

Figure 2. Schematic and photograph of the experimental setup showing the zero point three millimeter wire attachment used to secure the elastomeric modules

Evaluation of antibacterial properties

All procedures were conducted under aseptic conditions in triplicate within a laminar flow hood (Labconco). The bacterial strains selected were Streptococcus mutans ATCC au359 and Streptococcus sobrinus ATCC 27607, sourced from the Center for Research and Development in Health Sciences at the Autonomous University of Nuevo León (UANL). The strains were pre-cultured in Brain Heart Infusion (BHI) and trypticasein broth at 37 °C for 24 hours according to the supplier's recommended growth curves, then adjusted to a density of 1×10^{6}

cells/mL, equivalent to a McFarland standard of 0.0033. Three bacterial suspensions were prepared: one containing S. mutans, one with S. sobrinus, and a mixture of both. Aliquots of 100 microliters were placed in Eppendorf tubes, and three elastomeric modules from each experimental coating were immersed in each suspension. Samples were incubated at 37 °C for 24 hours. After incubation, each module was transferred to a fresh tube containing 1 mL of sterile water, vortexed for 20 seconds, and serially diluted. From the fifth dilution, 100 microliters were plated on Mitis Salivarius agar (MSA) and incubated for 24 hours at 37 °C to allow colony formation, after which CFUs were counted.

Assessment of cell viability

To determine cytocompatibility, CS- and CS-GTA-coated modules were placed in wells containing primary gingival fibroblasts (ATCC PCS-201-018) at a density of 10,000 cells per 100 µL of culture medium (DMEM) per well and incubated for 24 hours. The MTT assay was performed by adding 100 µL of 0.25 mg/mL MTT solution to each well and incubating for 4 hours under standard conditions. After incubation, 100 µL of dimethyl sulfoxide (DMSO) was added to dissolve the formazan crystals. Absorbance was measured at 570 nm using an iMark microplate reader (Bio-Rad Laboratories, Hercules, CA, USA). Uncoated EMs served as the positive control, while 0.12% chlorhexidine gluconate (CHX) served as the negative control. Cell viability was quantified based on the reduction of MTT to formazan. All tests were repeated five times, and statistical evaluation was performed using the Kolmogorov–Smirnov and Kruskal–Wallis tests.

Statistical evaluation

Mechanical testing data and antibacterial results were analyzed via one-way analysis of variance (ANOVA) using Jamovi software (version 2.6.44). Group comparisons were conducted using Tukey's post hoc test. Cell viability data were assessed with Kolmogorov–Smirnov and Kruskal–Wallis tests. A p-value of less than 0.05 was considered statistically significant for all analyses.

Results and Discussion

Physicochemical and mechanical characterization

FTIR spectra were recorded for the elastomeric modules coated with CS, CS-GTA, and for the uncoated control group **(Figure 3)**. Both CS and CS-GTA coatings showed a prominent band at 3332 cm^{-1}, which corresponds to the stretching vibrations of $–NH_2$ and O–H groups. Peaks at 2873 and 2954 cm^{-1} were attributed to C–H stretching. A band at 1595 cm^{-1} indicated the presence of C=O groups, while the 1061 cm^{-1} band corresponded to C–N stretching. Additionally, the peak at 1414 cm^{-1} represented the amide II C–N bond vibration, and the band at 3334 cm^{-1} reflected O–H and N–H stretching of alkyl (CH) groups. Signals at 1309 and 1725 cm^{-1} indicated the degree of deacetylation. The 1596 cm^{-1} peak was linked to amide I stretching from non-deacetylated residues, while the 1413 cm^{-1} and 1361 cm^{-1} bands corresponded to O–H vibrations of amide I and CH_3 groups, respectively. The 1462 cm^{-1} band was characteristic of amide II C–N stretching, and the region between 1530 and 815 cm^{-1} reflected C–O stretching within chitosan. No major spectral differences were observed between pure CS and CS-GTA; however, slight shifts occurred at 2918 and 2951 cm^{-1}, moving to 2925 and 2945 cm^{-1}, likely due to symmetrical CH_3 stretching. In contrast, the uncoated modules exhibited peaks at 962 and 1394 cm^{-1}, corresponding to CH_3 symmetrical stretching, which were absent in the coated samples.

Raman spectra are presented in **Figure 4**. The chitosan coating displayed a band at 2925 cm^{-1}, associated with $\nu(CH_2)$ stretching, and a peak at 1616 cm^{-1}, attributed to $\delta(NH_2)$ bending in the plane. Additional bands at 865 and 1184 cm^{-1} were assigned to C–C–O stretching vibrations. In the CS-GTA crosslinked coatings, a distinct band appeared at 638 cm^{-1}, reflecting C–C–C skeletal bending or deformation within the glutaraldehyde aliphatic chain. A peak at 1729 cm^{-1} indicated C=O stretching, while the 1616 cm^{-1} band corresponded to C=N stretching. Finally, the 1537 cm^{-1} peak was associated with C=C vibrations.

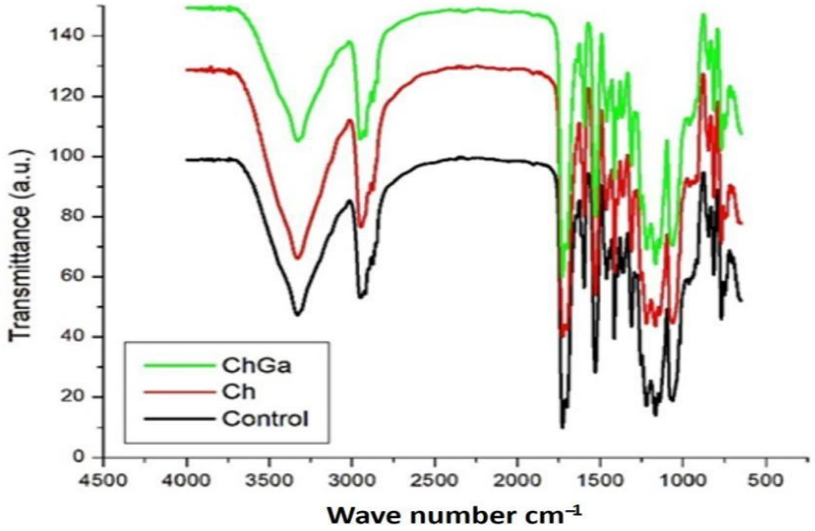

Figure 3. FTIR spectrum of the elastomeric modules

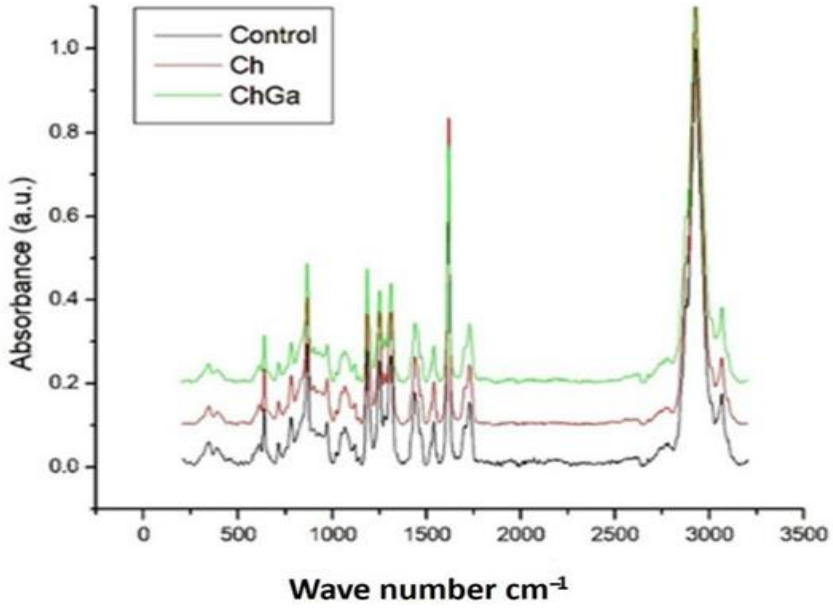

Figure 4. Raman spectroscopies of elastomeric module coatings

Mechanical characterization

The mechanical performance of the elastomeric modules, both coated and uncoated, is presented in **Table 1** and **Figure 5**. For yield strain (YS), the control modules reached an average of 336 ± 14.4 percent, whereas CS-coated modules measured 324 ± 18%, and the CS-GTA group showed 314 ± 11.3%. Statistical analysis using ANOVA indicated overall differences between the materials, and Tukey's post hoc test revealed that this difference was significant only between the control and the CS-GTA group.

Yield stress (σY) values were 5.06 ± 0.31 kPa for the control, 4.93 ± 0.26 kPa for the CS coating, and 4.74 ± 0.22 kPa for the CS-GTA group. ANOVA followed by Tukey testing showed no statistically significant differences among these groups.

Regarding maximum deformation (MD), uncoated modules exhibited 409 ± 11.9%, CS-coated modules 398 ± 4.1%, and CS-GTA modules 393 ± 18.5%. No significant differences were detected among the groups according to ANOVA. Maximum stress (σmax) results showed averages of 5.12 ± 0.28 kPa for the control, 4.94 ± 0.26 kPa for CS, and 4.82 ± 0.24 kPa for CS-GTA. While ANOVA did not show overall significant differences, the Tukey test identified a significant difference between the control and CS-GTA modules.

Table 1. Tensile mechanical properties of the elastomeric modules

Material	YS * (%)		σ_Y (MPa)	MD (%)	σ_{max} (MPa)
Uncoated	336 ± 14.4	a	5.06 ± 0.31	409 ± 11.9	5.12 ± 0.28
CS	324 ± 18	ab	4.93 ± 0.26	398 ± 14.1	4.94 ± 0.26
CS-GTA	314 ± 11.3	b	4.74 ± 0.22	393 ± 18.5	4.82 ± 0.24

CS = Chitosan; GTA = glutaraldehyde. Groups that do not share letters are statistically different from each other. YS = Yield Strain, σ_Y = Yield Stress, MD = Maximum Deformation, σ_{max} = Maximum Stress. * *p*-value < 0.05. a b indicate a significant difference between groups.

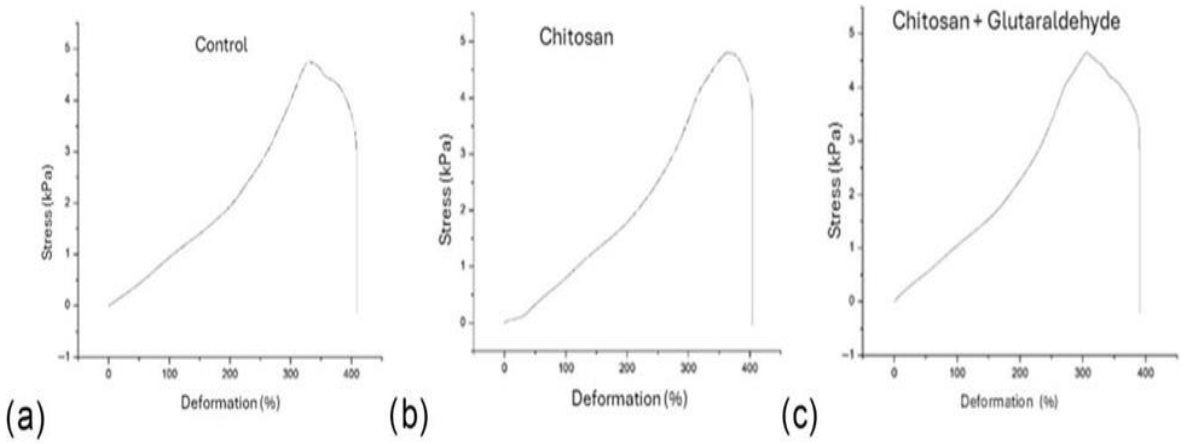

Figure 5. Representative stress–strain curves from tensile testing of elastomeric modules: (a) uncoated, (b) coated with CS, and (c) coated with CS-GTA

Antibacterial activity assay

All coated elastomeric modules showed a notable decrease in colony-forming units (CFUs) across the different bacterial suspensions **(Figure 6)**. Statistical analysis using ANOVA indicated significant differences among the groups for each bacterial composition. Tukey's post hoc test confirmed that CFU reductions differed significantly between the uncoated and coated modules. However, no statistically significant difference was observed between CS-coated and CS-GTA-coated modules for any bacterial composition. The lowest bacterial counts were observed for the CS-GTA-coated modules when exposed to the S. mutans + S. sobrinus mixture, followed by the CS-coated modules tested with S. mutans alone. Overall, both CS and CS-GTA coatings demonstrated comparable antimicrobial effects, which were markedly more effective than the uncoated modules across all bacterial conditions **(Table 2)**.

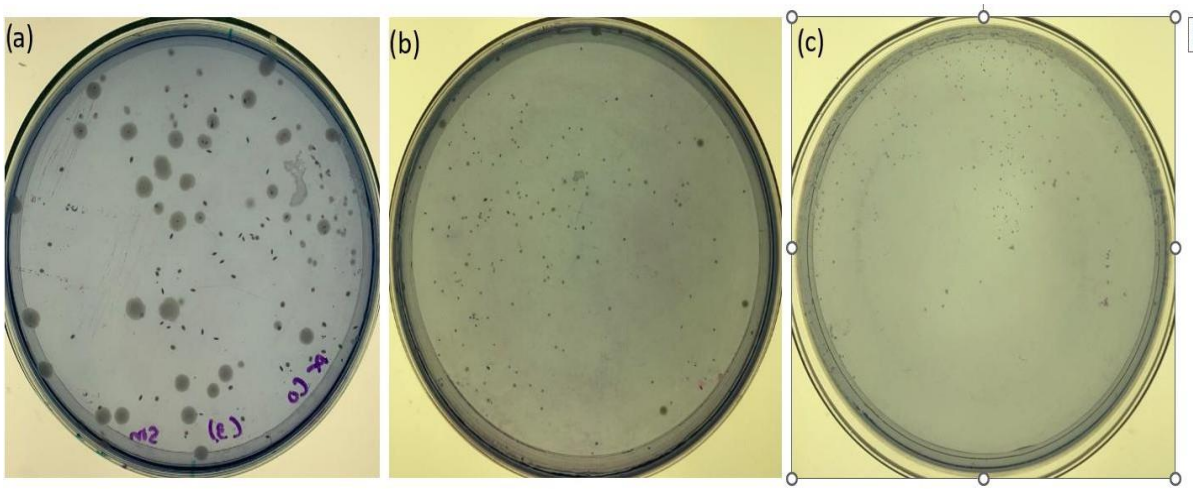

Figure 6. Photographs of Petri dishes illustrating the antibacterial effects of (a) uncoated control modules, (b) chitosan-coated modules, and (c) chitosan–glutaraldehyde-coated modules

Table 2. CFU values and standard deviations of the experimental coatings

Experimental Coatings	*S. mutans*	*S. sobrinus*	*S. sobrinus* + *S. mutans*
Ch			
Mean	208	906.666667	1544
SD	60.39867548	154.108187	421.729771
CS-GTA			
Mean	645.3333333	528	316
SD	184.2751566	276.781502	150.359569
Control			
Mean	733.3333333	1116	1368.333333
SD	110.01	86.0697392	165.9889555

Cell viability

The uncoated elastomeric modules were used as the reference, with their average absorbance representing 100 percent cell viability. The CS-coated modules exhibited an average viability of 85%, while the CS-GTA-coated modules showed 89% **(Figure 7)**. Since the data were not normally distributed, the Kruskal–Wallis test was applied to compare all four groups, revealing a statistically significant difference. Pairwise comparisons using the Mann–Whitney U test indicated that the only statistically significant difference occurred between the chlorhexidine group and the uncoated control. No significant differences were observed among the remaining groups after adjustment for multiple comparisons. Specifically, comparisons between CS and CS-GTA, as well as between CS-GTA and the uncoated modules, showed no significant variation. However, a significant reduction in cell viability was detected when comparing CS-coated modules to the uncoated control. This difference is visually represented in **Figure 7**.

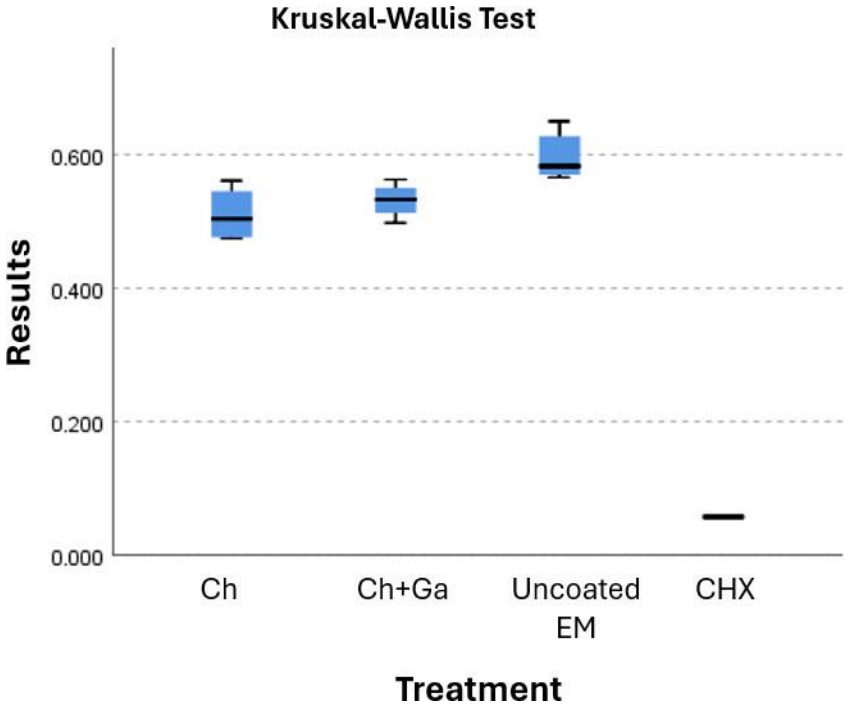

Figure 7. Cell viability of coated and uncoated elastomeric modules

Infrared spectroscopy confirmed that the elastomeric modules were successfully coated in both the CS and CS-GTA groups, consistent with the findings of Li *et al.* [20]. As reported by Tamer *et al.*, notable changes in FTIR spectra were observed within the 3200–3600 cm^{-1} range [31]. The introduction of GTA as a crosslinking agent produced detectable spectral modifications [32], although Monteiro *et al.* did not observe significant alterations in CS-GTA analyses [33]. In the present study, bands at 1309 and 1725 cm^{-1}, associated with the degree of deacetylation, align with the findings of Beppu *et al.* and Ki-Jae [34, 35], highlighting the relevance of deacetylation in modifying CS properties and behavior [36]. Other spectral bands identified in the experimental coatings, particularly in the 3400–3200 cm^{-1} region corresponding to O–H and N–H stretching, are consistent

with the observations of Cusihuamán *et al.* [21, 23, 32]. Escobar-Sierra *et al.* reported that the 2947 cm^{-1} band arises from alkyl (CH) groups [36], while additional FTIR analyses have linked the 1400–1600 cm^{-1} region to primary and secondary amides, in agreement with the present findings [31, 34, 37].

Raman spectroscopy further confirmed these results. Ren *et al.* identified characteristic C–H bonds at 895 and 1146 cm^{-1} [38], comparable to the peaks observed at 865 and 1184 cm^{-1} in this study, representing C–C–O stretching vibrations as reported by Gamboa-Solana [31]. Similarly, Mai *et al.* detected a primary CS signal at 680 cm^{-1}, close to the 693 cm^{-1} peak observed here [39].

Several studies have explored the mechanical properties of elastomeric materials in dentistry and orthodontics, alongside attempts to enhance their antimicrobial activity. For instance, Berni Osorio *et al.* found that immersion in 2% glutaraldehyde did not alter the mechanical behavior of elastomeric ligatures [40], which contrasts with the modifications observed in this study when GTA crosslinking was applied [41]. Melo-Pithon *et al.* evaluated multiple sterilization methods—including alcohol, autoclaving, ultraviolet light, peracetic acid, and glutaraldehyde—on elastic chains, reporting that ultraviolet treatment was the least effective, while other immersion methods did not compromise mechanical properties [42]. Stevenson *et al.* suggested that significant changes in elastomer mechanics require alterations in acidity, oxygen exposure, or temperature [43], which may explain why immersion in acidic GTA solutions influenced some material properties in this study.

Specifically, exposure to GTA-containing acidic medium slightly reduced yield stress (YS) but did not compromise the overall mechanical performance of the elastomeric modules. This aligns with the observations of Branco-Losito *et al.*, who reported no significant mechanical differences after immersion in chitosan or peracetic acid solutions [44]. Evangelista *et al.* noted that prolonged exposure to disinfectant liquids (over one hour) could negatively impact mechanical properties [10], and Terheyden *et al.* demonstrated that polyurethane ligatures resist mechanical degradation best, with ethylene oxide sterilization proving most effective [45]. Maximum deformation values in the current study were similar to those reported by Jeon *et al.*, showing no notable differences [4], while McKamey *et al.* found that applying a chlorine-substituted poly(para-xylylene) coating improved mechanical performance of elastic chain modules [46].

It is well-documented that mechanical properties of elastomeric ligatures can vary with color [8, 11, 47, 48]; this is why transparent modules were selected in the present study, which may be considered a limitation. Moreover, elastomeric mechanical behavior is influenced by moisture, as Halimi *et al.* reported differences between modules exposed and unexposed to artificial saliva [49]. Time-dependent mechanical degradation also affects elastomer capacity [50], and given that modules are typically replaced every four weeks, future research should investigate potential long-term changes in mechanical performance [51].

It is important to note that isolated bacterial strains were used in this study, and no significant differences in bacterial growth were observed. Kamarudin *et al.* employed a similar methodology and demonstrated the effectiveness of elastomers coated with chlorhexidine (CHX) for prolonged antimicrobial release [52]. Another study also reported favorable results for CHX coatings on elastomers, showing antimicrobial activity without negatively affecting mechanical performance [14]. Similarly, Uysal *et al.* highlighted the antimicrobial benefits of incorporating chitosan into toothpaste to reduce white spot lesions in patients undergoing orthodontic treatment [27].

The literature presents mixed outcomes regarding the efficacy of different antimicrobial agents, consistent with the present findings. For example, Benson *et al.* investigated fluoridated elastomeric ligatures but found them ineffective in limiting oral bacterial growth [53], and Doherty *et al.* reported that fluoride-releasing modules with sustained release did not provide anticariogenic benefits [54]. Likewise, the use of silver-coated elastomers has been explored, yet no significant antimicrobial effects were observed [55]. In contrast, the current study successfully applied chitosan coatings to elastomeric modules, though questions regarding their long-term stability and sustained efficacy remain and require further research.

It is also worth noting that adding a coating is only one factor influencing the mechanical behavior of elastomeric modules. The cell viability results support the biocompatibility of the coatings, with the CS-GTA crosslinked group exhibiting slightly higher viability compared to the CS-only coating.

Creating an in vitro environment with two or more bacterial strains better mimics natural oral biofilm conditions. Sharma *et al.* reported that the color of elastomeric ligatures can affect microbial adhesion [8], while Shi *et al.* demonstrated the effectiveness of chitosan as a scaffold for controlled drug release [56]. Similarly, Garner *et al.* confirmed the potential of chitosan nanoparticles as a silicone coating against C. albicans [57]. Padois *et al.* produced orthodontic polyurethane chains with a CH-loaded layer, achieving comparable antimicrobial outcomes

[58], and D'Almeida *et al.* observed antibacterial effects of chitosan coatings against S. epidermis [26]. Sarasam *et al.* also developed chitosan matrices that successfully inhibited S. mutans growth, although they were less effective against A. actinomycetemcomitans [59].

Conversely, other studies have shown limited antimicrobial effects with different agents. Doherty *et al.* found that prolonged fluoride release from elastomers did not prevent caries [56], and Kim *et al.* reported no significant antibacterial effect from silver-coated modules [57]. These results underscore that cariogenic bacteria may respond differently and independently.

Cytotoxicity studies indicate that chitosan exhibits low toxicity. Frigaard *et al.* demonstrated minimal cytotoxicity of chitosan nanoparticles [60], and Raviña *et al.* found that chitosan-g-poly(ethylene glycol) nanoparticles effectively delivered gene molecules without harmful effects [61]. The oral cavity has been identified as a safe site for chitosan nanoparticle application, and these nanoparticles have also shown selective cytotoxicity against cancer cells without affecting normal cells. Factors such as pH may influence cytotoxicity, warranting further investigation [62].

Additional in vitro MTT assays with chitosan and its derivatives confirm low toxicity compared to other antimicrobial agents, such as chlorhexidine (CHX), which has documented cytotoxic effects on human fibroblasts, myoblasts, and osteoblasts [63–66]. According to ISO 10993-5 [67], materials are considered non-cytotoxic if cell viability exceeds 70 percent. In this study, chitosan-based coatings achieved cell viability above 85%, indicating they are biocompatible and suitable for potential intraoral applications.

Conclusion

Chitosan (CS) coatings, both alone and crosslinked with glutaraldehyde (GTA), were successfully applied to elastomeric modules without substantially compromising their mechanical properties. Although the addition of GTA caused a minor decrease in yield stress, the overall mechanical performance of the modules remained satisfactory.

It should be emphasized that factors such as long-term durability of the coatings, environmental conditions including humidity, temperature, pH, and potential color changes in the elastomers were not examined in this study and warrant further investigation in future research.

Regarding antimicrobial efficacy, both CS and CS-GTA coatings effectively inhibited the growth of S. mutans, S. sobrinus, and their combined cultures, with no significant difference observed between the two coatings. This study focused on bacterial strains primarily associated with dental caries; thus, additional research is needed to evaluate the effects on other oral microorganisms.

Finally, both experimental coatings demonstrated acceptable levels of cell viability and, when compared to chlorhexidine, provided strong antimicrobial activity while maintaining biocompatibility. These findings indicate that chitosan-based coatings are a promising approach to reducing bacterial colonization on orthodontic elastomeric modules without negatively affecting their mechanical integrity.

Acknowledgments: None

Conflict of interest: None

Financial support: None

Ethics statement: None

References

1. Lamont RJ, Hajishengallis GN, Koo H, Jenkinson HF. Oral Microbiology and Immunology. Hoboken, NJ, USA: ASM Books; Wiley; 2019. ISBN 978-1-68367-290-6.
2. Perkowski K, Baltaza W, Conn DB, Marczyńska-Stolarek M, Chomicz L. Examination of oral biofilm microbiota in patients using fixed orthodontic appliances in order to prevent risk factors for health complications. Ann Agric Environ Med. 2019;26(2):231–5. doi:10.26444/aaem/105797.

3. Mummolo S, Nota A, Albani F, Marchetti E, Gatto R, Marzo G, et al. Salivary levels of Streptococcus mutans and Lactobacilli and other salivary indices in patients wearing clear aligners versus fixed orthodontic appliances: an observational study. PLoS ONE. 2020;15(3):e0228798. doi:10.1371/journal.pone.0228798.
4. Jeon HS, Jung EH, Kang SM, Lee ES, Lee JW, Kim BI. Improving the efficacy of chlorhexidine-releasing elastomerics using a layer-by-layer coating technique. Dent Mater J. 2017;36(4):476–81. doi:10.4012/dmj.2016-337.
5. Migliorati M, Isaia L, Cassaro A, Rivetti A, Silvestrini-Biavati F, Gastaldo L, et al. Efficacy of professional hygiene and prophylaxis on preventing plaque increase in orthodontic patients with multibracket appliances: a systematic review. Eur J Orthod. 2015;37(3):297–307. doi:10.1093/ejo/cju044.
6. Sundararaj D, Venkatachalapathy S, Tandon A, Pereira A. Critical evaluation of incidence and prevalence of white spot lesions during fixed orthodontic appliance treatment: a meta-analysis. J Int Soc Prev Community Dent. 2015;5(6):433–9. doi:10.4103/2231-0762.167719.
7. Proffit WR. Contemporary Orthodontics. Amsterdam, The Netherlands: Mosby Elsevier; 2007. ISBN 978-0-323-04613-8.
8. Sharma R, Sharma K, Sawhney R. Evidence of variable bacterial colonization on coloured elastomeric ligatures during orthodontic treatment: an intermodular comparative study. J Clin Exp Dent. 2018;10(3):e271–8. doi:10.4317/jced.54610.
9. Patano A, Malcangi G, Inchingolo AD, Garofoli G, De Leonardis N, Azzollini D, et al. Mandibular crowding: diagnosis and management—a scoping review. J Pers Med. 2023;13(5):774. doi:10.3390/jpm13050774.
10. Evangelista MB, Berzins DW, Monaghan P. Effect of disinfecting solutions on the mechanical properties of orthodontic elastomeric ligatures. Angle Orthod. 2007;77(4):681–7. doi:10.2319/052806-213.
11. Nakhaei S, Agahi RH, Aminian A, Rezaeizadeh M. Discoloration and force degradation of orthodontic elastomeric ligatures. Dent Press J Orthod. 2017;22(2):45–54. doi:10.1590/2177-6709.22.2.045-054.oar.
12. Forsberg CM, Brattström V, Malmberg E, Nord CE. Ligature wires and elastomeric rings: two methods of ligation, and their association with microbial colonization of Streptococcus mutans and Lactobacilli. Eur J Orthod. 1991;13(5):416–20. doi:10.1093/ejo/13.5.416.
13. Brêtas SM, Macari S, Elias AM, Ito IY, Matsumoto MAN. Effect of 0.4% stannous fluoride gel on Streptococci mutans in relation to elastomeric rings and steel ligatures in orthodontic patients. Am J Orthod Dentofacial Orthop. 2005;127(4):428–33. doi:10.1016/j.ajodo.2003.12.024.
14. Jeon HS, Choi CH, Kang SM, Kwon HK, Kim BI. Chlorhexidine-releasing orthodontic elastomerics. Dent Mater J. 2015;34(3):321–6. doi:10.4012/dmj.2014-216.
15. Hernández-Gómora AE, Lara-Carrillo E, Robles-Navarro JB, Scougall-Vilchis RJ, Hernández-López S, Medina-Solís CE, et al. Biosynthesis of silver nanoparticles on orthodontic elastomeric modules: evaluation of mechanical and antibacterial properties. Molecules. 2017;22(9):1407. doi:10.3390/molecules22091407.
16. Husain S, Al-Samadani KH, Najeeb S, Zafar MS, Khurshid Z, Zohaib S, Qasim SB. Chitosan biomaterials for current and potential dental applications. Materials. 2017;10(6):602. doi:10.3390/ma10060602.
17. Ayala Valencia G. Efecto antimicrobiano del quitosano: una revisión de la literatura. Sci Agroaliment. 2015;2(1):32–8.
18. Chuc Gamboa MG. Efecto de la modificación química y térmica en las propiedades de andamios de quitosano para regeneración ósea. Doctoral dissertation, Centro de Investigación Científica de Yucatán (CICY), Merida, Mexico; 2020.
19. Agnihotri SA, Mallikarjuna NN, Aminabhavi TM. Recent advances on chitosan-based micro- and nanoparticles in drug delivery. J Control Release. 2004;100(1):5–28. doi:10.1016/j.jconrel.2004.08.010.
20. Li B, Shan CL, Zhou Q, Fang Y, Wang YL, Xu F, Han LR, Ibrahim M, et al. Synthesis, characterization, and antibacterial activity of cross-linked chitosan-glutaraldehyde. Mar Drugs. 2013;11(5):1534–52. doi:10.3390/md11051534.
21. Cusihuamán Noa S, Talavera Núñez ME, Arenas Chávez C, Pacheco Salazar DG, Vera Gonzales C. Caracterización por técnicas espectroscópicas del O-carboximetilquitosano obtenido por derivatización del quitosano. Rev Soc Química Perú. 2018;84:204–16.
22. Cánepa Ivazeta JL. Obtención de quitosanas con alto grado de desacetilación. Lima, Peru: Pontificia Universidad Católica del Perú; 2018.
23. Curbelo Hernández C, Palacio Dubois Y, Fanego Hernández S. Desacetilación de quitina obtenida por vía química de exoesqueletos de camarón Litopenaeus vannamei. Cent Azúcar. 2021;48:53–61.

24. Yu Q, Song Y, Shi X, Xu C, Bin Y. Preparation and properties of chitosan derivative/poly(vinyl alcohol) blend film crosslinked with glutaraldehyde. Carbohydr Polym. 2011;84(2):465–70. doi:10.1016/j.carbpol.2010.12.006.
25. Dutta PK, Tripathi S, Mehrotra GK, Dutta J. Perspectives for chitosan based antimicrobial films in food applications. Food Chem. 2009;114(4):1173–82. doi:10.1016/j.foodchem.2008.11.047.
26. D'Almeida M, Attik N, Amalric J, Brunon C, Renaud F, Abouelleil H, Toury B, Grosgogeat B. Chitosan coating as an antibacterial surface for biomedical applications. PLoS ONE. 2017;12(11):e0189537. doi:10.1371/journal.pone.0189537.
27. Uysal T, Akkurt MD, Amasyali M, Ozcan S, Yagci A, Basak F, Sagdic D. Does a chitosan-containing dentifrice prevent demineralization around orthodontic brackets? Angle Orthod. 2011;81(2):319–25. doi:10.2319/062910-359.1.
28. Sehmi SK, Allan E, MacRobert AJ, Parkin I. The bactericidal activity of glutaraldehyde-impregnated polyurethane. MicrobiologyOpen. 2016;5(6):891–7. doi:10.1002/mbo3.378.
29. Jayakrishnan A, Jameela SR. Glutaraldehyde as a fixative in bioprostheses and drug delivery matrices. Biomaterials. 1996;17(6):471–84. doi:10.1016/0142-9612(96)82721-9.
30. Berridge MV, Herst PM, Tan AS. Tetrazolium dyes as tools in cell biology: new insights into their cellular reduction. In: Biotechnology Annual Review. Amsterdam, The Netherlands: Elsevier; 2005. p. 127–52. ISBN 1387-2656.
31. Gamboa Solana CDC. Actividad antimicrobiana de películas de quitosano modificado. Maestría Thesis, Universidad Autónoma de Yucatán, Merida, Mexico; 2020.
32. Valizadeh S, Naseri M, Babaei S, Hosseini SMH, Imani A. Development of bioactive composite films from chitosan and carboxymethyl cellulose using glutaraldehyde, cinnamon essential oil and oleic acid. Int J Biol Macromol. 2019;134:604–12. doi:10.1016/j.ijbiomac.2019.05.071.
33. Monteiro OA, Airoldi C. Some studies of crosslinking chitosan-glutaraldehyde interaction in a homogeneous system. Int J Biol Macromol. 1999;26:119–28. doi:10.1016/s0141-8130(99)00068-9.
34. Beppu MM, Vieira RS, Aimoli CG, Santana CC. Crosslinking of chitosan membranes using glutaraldehyde: effect on ion permeability and water absorption. J Membr Sci. 2007;301:126–30. doi:10.1016/j.memsci.2007.06.015.
35. Jeong KJ, Song Y, Shin HR, Kim JE, Kim J, Sun F, et al. In vivo study on the biocompatibility of chitosan-hydroxyapatite film depending on degree of deacetylation. J Biomed Mater Res A. 2017;105:1637–45. doi:10.1002/jbm.a.35993.
36. Escobar-Sierra DM, Perea-Mesa YP. Manufacturing and evaluation of chitosan, PVA and aloe vera hydrogels for skin applications. Dyna. 2017;84:134–42.
37. Bujňáková Z, Dutková E, Zorkovská A, Baláž M, Kováč J, Kello M, et al. Mechanochemical synthesis and in vitro studies of chitosan-coated InAs/ZnS mixed nanocrystals. J Mater Sci Mater Med. 2017;52:721–35. doi:10.1007/s10853-016-0366-x.
38. Ren XD, Liu QS, Feng H, Yin XY. The characterization of chitosan nanoparticles by Raman spectroscopy. Appl Mech Mater. 2014;665:367–70.
39. Mai TTT, Ha PT, Pham HN, Le TTH, Pham HL, Phan TBH, et al. Chitosan and O-carboxymethyl chitosan modified Fe3O4 for hyperthermic treatment. Adv Nat Sci Nanosci Nanotechnol. 2012;3:015006.
40. Berni Osorio L, Makito Osawa Gutierrez L, Martinelli de Lima E, Gonçalves Mota E, Macedo de Menezes L. Disinfection of orthodontic elastomers and its effects on tensile strength. Turk J Orthod. 2022;35:22–6. doi:10.5152/TurkJOrthod.2022.20151.
41. Eliades T, Eliades G, Silikas N, Watts DC. In vitro degradation of polyurethane orthodontic elastomeric modules. J Oral Rehabil. 2005;32:72–7. doi:10.1111/j.1365-2842.2004.01366.x.
42. Pithon MM, Ferraz CS, Rosa FCS, Rosa LP. Sterilizing elastomeric chains without losing mechanical properties. Is it possible? Dent Press J Orthod. 2015;20:96–100. doi:10.1590/2176-9451.20.3.096-100.oar.
43. Stevenson JS, Kusy RP. Structural degradation of polyurethane-based elastomeric modules. J Mater Sci Mater Med. 1995;6:377–84. doi:10.1007/BF00120277.
44. Losito KAB, Lucato AS, Tubel CAM, Correa CA, Santos JCB. Force decay in orthodontic elastomeric chains after immersion in disinfection solutions. Braz J Oral Sci. 2014;13:266–9.

45. Terheyden H, Lee U, Ludwig K, Kreusch T, Hedderich J. Sterilization of elastic ligatures for intraoperative mandibulomaxillary immobilization. Br J Oral Maxillofac Surg. 2000;38:299–304. doi:10.1054/bjom.1999.0237.
46. McKamey RP, Whitley JQ, Kusy RP. Physical and mechanical characteristics of a chlorine-substituted poly(para-xylylene) coating on orthodontic chain modules. J Mater Sci Mater Med. 2000;11:407–19. doi:10.1023/a:1008983808008.
47. Lam TV, Freer TJ, Brockhurst PJ, Podlich HM. Strength decay of orthodontic elastomeric ligatures. J Orthod. 2002;29:37–43. doi:10.1093/ortho/29.1.37.
48. Antony PJ, Paulose J. An in-vitro study to compare the force degradation of pigmented and non-pigmented elastomeric chains. Indian J Dent Res. 2014;25:208–13.
49. Halimi A, Azeroual M-F, Doukkali A, El Mabrouk K, Zaoui F. Elastomeric chain force decay in artificial saliva: an in vitro study. Int Orthod. 2013;11:60–70. doi:10.1016/j.ortho.2012.12.007.
50. Dowling PA, Jones WB, Lagerstrom L, Sandham JA. An investigation into the behavioural characteristics of orthodontic elastomeric modules. Br J Orthod. 1998;25:197–202. doi:10.1093/ortho/25.3.197.
51. Datana S, Sengupta J, Sharma V. Structural and mechanical characterization of newer elastomeric modules. J Ind Orthod Soc. 2006;39:23–9.
52. Kamarudin Y, Skeats MK, Ireland AJ, Barbour ME. Chlorhexidine hexametaphosphate as a coating for elastomeric ligatures with sustained antimicrobial properties: a laboratory study. Am J Orthod Dentofac Orthop. 2020;158:e73–82. doi:10.1016/j.ajodo.2020.07.027.
53. Benson PE, Douglas CWI, Martin MV. Fluoridated elastomers: effect on the microbiology of plaque. Am J Orthod Dentofac Orthop. 2004;126:325–30. doi:10.1016/j.ajodo.2003.07.007.
54. Doherty UB, Benson PE, Higham SM. Fluoride-releasing elastomeric ligatures assessed with the in situ caries model. Eur J Orthod. 2002;24:371–8. doi:10.1093/ejo/24.4.371.
55. Kim YJ, Lee DY, Lee JY, Lim YK. The effect of silver ion-releasing elastomers on mutans streptococci in dental plaque. Korean J Orthod. 2012;42:87–93. doi:10.4041/kjod.2012.42.2.87.
56. Shi P, Zuo Y, Zou Q, Shen J, Zhang L, Li Y, Morsi YS. Improved properties of incorporated chitosan film with ethyl cellulose microspheres for controlled release. Int J Pharm. 2009;375:67–74. doi:10.1016/j.ijpharm.2009.04.016.
57. Garner SJ, Nobbs AH, McNally LM, Barbour ME. An antifungal coating for dental silicones composed of chlorhexidine nanoparticles. J Dent. 2015;43:362–72. doi:10.1016/j.jdent.2014.12.005.
58. Padois K, Bertholle V, Pirot F, Hyunh TTN, Rossi A, Colombo P, Falson F, et al. Chlorhexidine salt-loaded polyurethane orthodontic chains: in vitro release and antibacterial activity studies. AAPS PharmSciTech. 2012;13:1446–50. doi:10.1208/s12249-012-9872-6.
59. Sarasam AR, Brown P, Khajotia SS, Dmytryk JJ, Madihally SV. Antibacterial activity of chitosan-based matrices on oral pathogens. J Mater Sci Mater Med. 2008;19:1083–90. doi:10.1007/s10856-007-3072-z.
60. Frigaard J, Jensen JL, Galtung HK, Hiorth M. The potential of chitosan in nanomedicine: an overview of the cytotoxicity of chitosan based nanoparticles. Front Pharmacol. 2022;13:880377. doi:10.3389/fphar.2022.880377.
61. Raviña M, Cubillo E, Olmeda D, Novoa-Carballal R, Fernandez-Megia E, Riguera R, et al. Hyaluronic acid/chitosan-g-poly(ethylene glycol) nanoparticles for gene therapy: an application for pDNA and siRNA delivery. Pharm Res. 2010;27:2544–55. doi:10.1007/s11095-010-0263-y.
62. Zoe LH, David SR, Rajabalaya R. Chitosan nanoparticle toxicity: a comprehensive literature review of in vivo and in vitro assessments for medical applications. Toxicol Rep. 2023;11:83–106. doi:10.1016/j.toxrep.2023.06.012.
63. Zaboon MH, Saleh AA, Al-Lami HS. Synthesis, characterization and cytotoxicity investigation of chitosan-amino acid derivatives nanoparticles in human breast cancer cell lines. J Mex Chem Soc. 2021;65:178–88.
64. Anitha A, Rani VD, Krishna R, Sreeja V, Selvamurugan N, Nair S, Tamura H, et al. Synthesis, characterization, cytotoxicity and antibacterial studies of chitosan, O-carboxymethyl and N,O-carboxymethyl chitosan nanoparticles. Carbohydr Polym. 2009;78:672–7.
65. Ivanova N, Ermenlieva N, Simeonova L, Kolev I, Slavov I, Karashanova D, et al. Chlorhexidine-silver nanoparticle conjugation leading to antimicrobial synergism but enhanced cytotoxicity. Pharmaceutics. 2023;15:2298. doi:10.3390/pharmaceutics15092298.

66. Liu JX, Werner J, Kirsch T, Zuckerman JD, Virk MS. Cytotoxicity evaluation of chlorhexidine gluconate on human fibroblasts, myoblasts, and osteoblasts. J Bone Jt Infect. 2018;3:165–72. doi:10.7150/jbji.26355.
67. ISO 10993-5:2009. Biological evaluation of medical devices—part 5: tests for in vitro cytotoxicity. Geneva, Switzerland: International Organization for Standardization; 2009.